

Neomycin Binding to Watson–Hoogsteen (W–H) DNA Triplex Groove: A Model

Dev P. Arya,* Ljiljana Micovic, I. Charles, R. Lane Coffee, Jr., Bert Willis, and Liang Xue

Contribution from the Laboratory of Medicinal Chemistry, Department of Chemistry, Clemson University, Clemson, South Carolina 29634

Received July 18, 2002 E-mail: dparya@clemson.edu

Abstract: Neomycin is the most effective aminoglycoside (groove binder) in stabilizing a DNA triple helix. It stabilizes TAT, as well as mixed base DNA triplexes, better than known DNA minor groove binders (which usually destabilize the triplex) and polyamines. Neomycin selectively stabilizes the triplex (in the presence of salt), without any effect on the DNA duplex. (1) Triplex stabilization by neomycin is salt dependent (increased KCl and MgCl₂ concentrations decrease neomycin's effectiveness, at a fixed drug concentration). (2) Triplex stabilization by neomycin is pH dependent (increased pH decreases neomycin's effectiveness, at a fixed drug concentration). (3) CD binding studies indicate ~5–7 base triplets/drug apparent binding site, depending upon the structure/sequence of the triplex. (4) Neomycin shows nonintercalative groove binding to the DNA triplex, as evident from viscometric studies. (5) Neomycin shows a preference for stabilization of TAT triplets but can also accommodate CGC⁺ triplets. (6) Isothermal titration calorimetry (ITC) studies reveal an association constant of ~2 × 10⁵ M⁻¹ between neomycin and an intramolecular triplex and a higher K_a for polyA·2polydT. (7) Binding/modeling studies show a marked preference for neomycin binding to the larger W–H groove. Ring I/II amino groups and ring IV amines are proposed to be involved in the recognition process. (8) The novel selectivity of neomycin is suggested to be a function of its charge and shape complementarity to the triplex W–H groove, making neomycin the first molecule that selectively recognizes a triplex groove over a duplex groove.

Introduction

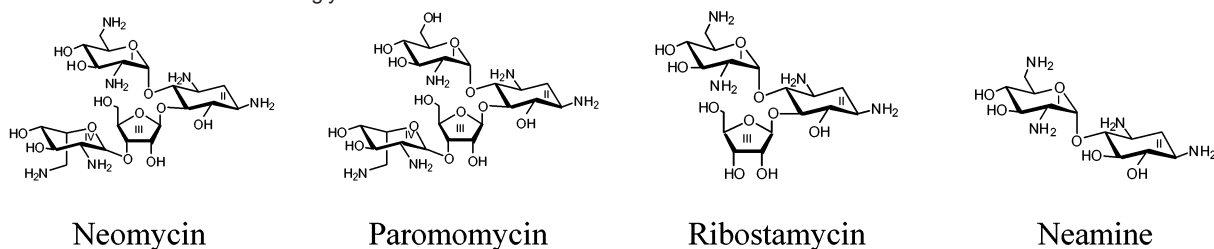
Recognition of duplex DNA by small molecules (minor groove binders—polyamides) and oligonucleotides (major groove binders—DNA triple helices) are promising approaches to a chemical solution for DNA recognition.¹ Triple helix formation has been the focus of considerable interest because of the possible applications in developing new molecular biology tools as well as therapeutic agents and because of the possible relevance of H-DNA structures in biological systems.^{2–6} Several intercalators as well as various DNA minor groove ligands have been shown to bind to DNA triple helices.^{5,7,8} Intercalators usually stabilize to a greater extent triple helices containing TAT triplets, whereas minor groove binders usually destabilize triplexes.⁹ In our quest for new ligands for triple helix

stabilization, we have investigated aminoglycoside antibiotics (Scheme 1).^{10–12}

The growing specter of antibiotic resistance has rekindled the need for better/less toxic antibiotics.¹³ Aminoglycosides have recently been the focus of various antiviral and antibacterial targeted studies.^{14–23} Triplex stabilization by aminoglycosides has been suggested to have implications in their range of toxicities, in conjunction with free radical based mechanisms.¹² The H-DNA prone sequences are abundant in eukaryotes, suggesting that binding to the bacterial ribosome may not be the only site of action for these compounds. Previous work by

- (1) Dervan, P. B. *Bioorg. Med. Chem.* **2001**, *9*, 2215–2235.
- (2) Kool, E. T. *Acc. Chem. Res.* **1998**, *31*, 502–510.
- (3) Kool, E. T. *New J. Chem.* **1997**, *21*, 33–45.
- (4) Frank-Kamenetskii, M. D.; Mirkin, S. M. *Annu. Rev. Biochem.* **1995**, *64*, 65–95.
- (5) Ganesh, K. N.; Kumar, V. A.; Barawkar, D. A. In *Supramolecular Control of structure and reactivity*; Hamilton, A. D., Ed.; John Wiley & Sons Ltd., 1996; pp 263–327.
- (6) Feigon, J.; Wang, E. In *Nucleic Acid Structure*, 1st ed.; Neidle, S., Ed.; Oxford University Press: Oxford, 1999; Vol. 1, pp 355–388.
- (7) Shafer, R. H. *Prog. Nucleic Acid Res. Mol. Biol.* **1998**, *59*, 55–94.
- (8) Escude, C.; Nguyen, C. H.; Kukreti, S.; Janin, Y.; Sun, J.-S.; Bisagni, E.; Garestier, T.; Helene, C. *Proc. Natl. Acad. Sci. U.S.A.* **1998**, *95*, 3591–3596.
- (9) Lane, A.; Jenkins, T. *Curr. Org. Chem.* **2001**, *5*, 845–869.

- (10) Arya, D. P.; Coffee, R. L., Jr. *Bioorg. Med. Chem. Lett.* **2000**, *10*, 1897–1899.
- (11) Arya, D. P.; Coffee, R. L., Jr.; Charles, I. *J. Am. Chem. Soc.* **2001**, *123*, 11093–11094.
- (12) Arya, D. P.; Coffee, R. L., Jr.; Willis, B.; Abramovitch, A. I. *J. Am. Chem. Soc.* **2001**, *123*, 5385–5395.
- (13) Henry, C. M. *C&E News* **2000**, *78*, 41–58.
- (14) Azucena, E.; Grapsas, I.; Mobashery, S. *J. Am. Chem. Soc.* **1997**, *119*, 2317–2318.
- (15) Azucena, E.; Mobashery, S. *Drug Resist. Updates* **2001**, *4*, 106–117.
- (16) Cho, J.; Rando, R. R. *Biochemistry* **1999**, *38*, 8548–8554.
- (17) Michael, K.; Wang, H.; Tor, Y. *Bioorg. Med. Chem.* **1999**, *7*, 1361–1371.
- (18) Suchek, S. J.; Greenberg, W. A.; Tolbert, T. J.; Wong, C.-H. *Angew. Chem., Int. Ed.* **2000**, *39*, 1080–1084.
- (19) Wang, H.; Tor, Y. *Angew. Chem., Int. Ed.* **1998**, *37*, 109–111.
- (20) Lacy, M. K.; Nicolau, D. P.; Nightingale, C. H.; Quintiliani, R. *Clin. Infect. Dis.* **1998**, *27*, 23–27.
- (21) Kotra, L. P.; Haddad, J.; Mobashery, S. *Antimicrob. Agents Chemother.* **2000**, *44*, 3249–3256.
- (22) Faber, C.; Sticht, H.; Schweimer, K.; Rosch, P. *J. Biol. Chem.* **2000**, *275*, 20660–20666.
- (23) Hermann, T. *Angew. Chem., Int. Ed.* **2000**, *39*, 1890–1905.

Scheme 1. Structures of Some Aminoglycoside Antibiotics^a

^a For a complete list, please see Supporting Information.

us and others also suggests that aminoglycoside binding may not be simply RNA specific but specific for nucleic acids that can adopt the A-conformation (RNA duplex,^{11,12,24} A-form DNA duplex,²⁵ DNA–RNA hybrid duplex,¹¹ DNA triplex,¹² and RNA triplex¹²).

There is a significant amount of high-resolution information on complexes of compounds that bind to both DNA and RNA by intercalation and on compounds that bind in the DNA minor groove.^{1,26} Good models exist for proteins and peptides that bind in the major groove of DNA and RNA.^{27–29} There is, however, little information available for antibiotics that selectively bind DNA triplex grooves or RNA triplex grooves. We have reported preliminary data narrowing this disparity between groove recognition of duplex versus triplex nucleic acids.^{11,12} We present neomycin as one of the first examples that bridge this gap and may thus lead to a novel understanding of the recognition principle(s) involved in selective targeting of triplex grooves. A fundamental understanding of aminoglycoside interaction with triplex nucleic acid structures is thus necessary to better understand aminoglycoside function as well as decipher the underlying principles in the long standing problem of selective triplex groove/backbone recognition.

Materials and Methods

The concentrations of nucleotide solutions were determined using the extinction coefficients (per mol of nucleotide) calculated according to the nearest neighbor method. The concentrations of all the polymer solutions were determined spectrophotometrically using the following extinction coefficients (in units of mol of nucleotide/L⁻¹ cm⁻¹): $\epsilon_{265} = 9000$ for polydT, $\epsilon_{260} = 6000$ for polydA·polydT, $\epsilon_{253} = 7400$ for polydG·polydC, $\epsilon_{274} = 7400$ for polydC; for the intramolecular triplex (per strand), 5'-dA₁₂-x-dT₁₂-x-dT₁₂-3', $\epsilon_{260} = 341\,100$; for the intramolecular triplex (per strand), 5'-AAAGAAAAGAAA-x-TTCTTTTCTTT-x-TTCTTTTCTTT-3', $\epsilon_{260} = 336\,100$, where x refers to hexaethylene glycol. Solutions of the intramolecular triplex were heated to 90 °C to ensure complete dissociation and were subsequently quantitated using UV absorbance. Intramolecular triplexes were synthesized as previously reported.³⁰ In all cases where mentioned, the term r_{db} refers to the molar ratio of drug-to-base.

UV Spectroscopy. All UV spectra were recorded on a Cary IE UV–vis spectrophotometer equipped with a thermoelectrically controlled 12 cell holder. Quartz cells with a 1 cm path length were used for all the absorbance studies. Spectrophotometer stability and λ alignment were checked prior to initiation of each melting point experiment. For

the T_m determinations, derivatives were used. Data were recorded every 1.0 °C. In all intramolecular triplex experiments, the samples were heated to 95 °C for 5 min and then cooled to 4 °C over 16 h. The temperature was raised in 0.2 °C/min increments. For all polynucleotide experiments, the samples were heated to 95 °C, followed by annealing at a rate of 0.2 °C/min and then melting at 0.2 °C/min. Samples were brought back to 20 °C after run. Absorbance versus temperature profiles were measured at 260, 280, and 284 nm.

CD Spectropolarimetry. All CD experiments were conducted at 20 °C on a JASCO J-810 spectropolarimeter equipped with a thermoelectrically controlled cell holder. A quartz cell with a 1 cm path length was used in the CD studies. CD spectra were recorded as an average of 3 scans from 200 to 350 nm with data recorded in 0.1 nm increments with an averaging time of 2 s. In CD melting experiments, samples were incubated at the starting temperature (10 °C) for 30 min prior to heating at a rate of 0.2 °C/min, with data collection at single degree increments. For isothermal titration experiments, small aliquots of concentrated drug solutions were added to a solution of DNA, inverted twice, and allowed to equilibrate for at least 10 min prior to scanning. For the intramolecular triplex, small aliquots (0.6–40 μ L) of a concentrated neomycin solution (500 μ M and 1000 μ M) were added to a 2 mL solution of 5'-dA₁₂-x-dT₁₂-x-dT₁₂-3' triplex solution (4 μ M/strand) and resulting CD spectra ($\lambda = 300$ –210 nm) were obtained after incubation for 10 min at 20 °C. The starting DNA solution was allowed to equilibrate at least 30 min prior to the first addition of drug. For the 22mer triplex, small aliquots (0.6–20.6 μ L) of a concentrated neomycin solution (500 μ M and 1000 μ M) were added to a 2 mL solution of dY₂₂dR₂₂dT₂₂ (1 μ M/strand) and resulting CD spectra ($\lambda = 330$ –210 nm) were obtained after incubation for 10 min at 15 °C.

Viscometry. Viscosity measurements were conducted using a Cannon-Ubbelohde 75 capillary viscometer which was submerged in a water bath maintained at 27 \pm 0.05 °C. Neomycin (2 mM) was titrated into a solution of DNA (100 μ M/base triplet, 1.03 mL), and flow times (from 111 to 104 s) were recorded in triplicate using a stopwatch, with a standard deviation \leq 0.1 s. All solutions were in buffer, which consisted of 10 mM sodium cacodylate, 0.5 mM EDTA, 150 mM KCl, and 2.5 mM MgCl₂ at pH 7.2.

Isothermal Titration Calorimetry (ITC). Isothermal calorimetric measurements were performed at 20 °C on a MicroCal VP-ITC (MicroCal, Inc.; Northampton, MA). In a typical experiment, 5 μ L aliquots of 500 μ M neomycin were injected from a 250 μ L rotating syringe (300 rpm) into an isothermal sample chamber containing 1.42 mL of an intramolecular DNA triplex solution that was 4 μ M/strand. Each experiment of this type was accompanied by the corresponding control experiment in which 5 μ L aliquots of 500 μ M drug were injected into a solution of buffer alone. The duration of each injection was 10 s, and the delay between injections was 300 s. The initial delay prior to the first injection was 60 s. Each injection generated a heat burst curve (microcalories per second vs seconds). The area under each curve was determined by integration using the Origin (version 5.0) software to obtain a measure of the heat associated with that injection. The heat associated with each drug–buffer injection was subtracted from the corresponding heat associated with each drug–DNA injection to yield the heat of drug binding for that injection.

(24) Chen, Q.; Shafer, R. H.; Kuntz, I. D. *Biochemistry* **1997**, *36*, 11402–11407.

(25) Robinson, H.; Wang, A. H. *Nucleic Acids Res.* **1996**, *24*, 676–682.

(26) Wemmer, D. E. *Annu. Rev. Biophys. Biomol. Struct.* **2000**, *29*, 439–461.

(27) Nagai, K. *Curr. Opin. Struct. Biol.* **1996**, *6*, 53–61.

(28) Wolfe, S. A.; Nekludova, L.; Pabo, C. O. *Annu. Rev. Biophys. Biomol. Struct.* **2000**, *29*, 183–212.

(29) Choo, Y.; Klug, A. *Curr. Opin. Struct. Biol.* **1997**, *7*, 117–125.

(30) Durand, M.; Chevré, K.; Chassignol, M.; Thuong, N. T.; Maurizot, J. C. *Nucleic Acids Res.* **1990**, *18*, 6353–6359.

Molecular Modeling. The structures of the dA₁₀·2dT₁₀ triplex, neomycin, and paromomycin structure have been built and optimized with the MacroModel program³¹ using the AMBER* force field.^{32,33} The all atom AMBER* force field was used, as it reproduces X-ray and NMR derived DNA structures. The continuum GB/SA model of water,^{34,35} as implemented in MacroModel, has been used in all calculations. The force field atomic charges were used for the triplex. The ligands were built and optimized in MacroModel, and the RESP charges were derived using ab initio calculations with the 6-31G* basis set in the Jaguar program.³¹ The structure of the dA₁₀·2dT₁₀ triplex was built starting from the experimental (NMR) solution structure of a structurally related DNA triplex.^{36,37} Twenty seven sodium ions were added to neutralize the structure at the beginning. The sodium ions were removed, and the structure was reoptimized to within a gradient of 0.05 kJ/mol Å. Only the movement of atoms of external bases were restricted during minimization. The structure of neomycin was built by MacroModel and submitted to conformational searching in order to find the global minimum structure and the other low energy conformations. For conformational searching, the Monte Carlo (MC) routine^{38,39} from MacroModel was used. Three MC runs (for all single bond torsional angles and 1000 steps each) starting from different initial conformations were done, yielding the same global minimum conformation. All the flexible bonds were selected.

Several of the lowest conformations of neomycin were manually docked to the DNA triplex groove in different orientations. The conformations of the molecules were adjusted to allow maximum base–ligand and phosphate–ligand H-bond formation with no significant unfavorable van der Waals interactions. Neomycin was manually docked into the triplex grooves, avoiding any unfavorable steric clashes, and positioned approximately centrally in the entrance to the grooves. For a more detailed analysis of ligand groove interactions, appropriate contacts between protonated amines and phosphate oxygens on the backbone were selected. The minimized complexes were then reminimized with the distance constraints removed to an RMS gradient of 0.08 kcal/mol Å to allow unfavorable contacts to be removed. In the next step, all the restrictions were removed except the movement of ring atoms of the terminal bases, and the structure was optimized to a gradient of 0.05 kJ/mol Å or lower. To test the stability of the complex, the low energy complexes were submitted to 500 ps MD simulations using reported procedures (stochastic dynamics, constant temperature of 300 K, with coupling constant of 0.2 ps, and a time step of 1.0 fs).³¹ The SHAKE procedure was used for all bonds. Electrostatic potential was generated from viewerLite 5.0 for Windows, Accelrys Inc., CA, USA using Gasteiger charges.

Results

1. Melting Curves and Aminoglycoside Structure–Activity Relationships. Melting studies of triplexes formed from short strand DNA homooligomers dA₁₆·2dT₁₆ as well as polynucleotides were carried out in the presence of aminoglycosides, using UV spectroscopy at 260/280 nm. All triplex melting curves exhibit hysteresis, whereas all duplex melting and annealing curves overlap. The divergence of the heating and cooling curves are functions of the rates of heating and cooling. Job plots were

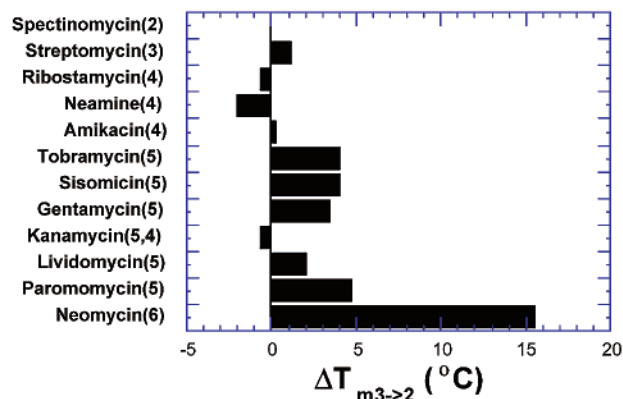


Figure 1. Change in $\Delta T_{m3\rightarrow2}$ ($r_{ab} = 0.67$), where r_{ab} = ratio of the drug/base triplet, on the stabilization of the polydA·2polydT triplex melt in the presence of 150 mM KCl. Without any aminoglycoside present, the melting temperature of the triplex was 34.0 °C. Buffer conditions: 10 mM sodium cacodylate, 0.5 mM EDTA, pH 7.2. The melting rate was 0.2 °C/min. Number of amines in each drug is shown in parentheses.

constructed from absorbances of respective oligomers in the presence of aminoglycosides to ensure the formation of triplex and duplex species at respective temperatures.

Our previous studies with the polynucleotide triplex have shown the remarkable effectiveness of neomycin in stabilizing the triplex without affecting the duplex T_m .¹² Nature has provided us antibiotics to allow for a simplified version of the aminoglycoside–triplex structure–activity relationship. A few aminoglycosides studied (Scheme 1) can be viewed as variations of neomycin. The triplex stabilization analysis (Figure 1) was used to build a model for the triplex–neomycin complex.

The following relationships are available from those studies: (i) paromomycin is much weaker in stabilizing the triplex (amino group in ring I is a key element in recognition); (ii) tobramycin, kanamycin, and gentamycin have a much weaker stabilizing effect (ribose, ring III, is important in providing the appropriate confirmation for neomycin binding); (iii) ribostamycin and neamine are much weaker in stabilizing the triplex and have a similar effect on triplex stabilization (ring IV amines are involved in recognition, and ring III could provide the neomycin conformer necessary for successful binding).

2. Salt/pH/Viscosity Effects in Neomycin Binding to a Polynucleotide DNA Triplex. A. Effect of KCl. At a fixed neomycin concentration, melting studies were carried out for the polydA·2polydT triplex with varying KCl concentration. As visible from Figure 2, increasing KCl concentration decreases the stabilization induced by neomycin. For the polynucleotide triplex, there is a decrease in $\Delta T_{m3\rightarrow2}$ from 16 °C (150 mM KCl) to 2 °C (250 mM KCl), in the presence of neomycin ($r_{ab} = 0.67$).

B. Effect of MgCl₂. At a fixed neomycin concentration, melting studies were carried out for the polydA·2polydT triplex in the presence of increasing MgCl₂ concentration. As visible from Figure 3, increasing neomycin concentration does not have a significant effect on polydA·2polydT triplex stabilization in the presence of 3mM MgCl₂. The effect of increasing MgCl₂ concentration is, however, much more dramatic than that observed with KCl.

C. Effect of pH. At a fixed neomycin concentration, melting studies were carried out for the polydA·2polydT triplex with increasing buffer pH. As visible from Figure 4, increasing the

- (31) Trent, J. O. *Methods Enzymol.* **2001**, *340*, 290–328.
 (32) Weiner, S. J.; Kollman, P. A.; Nguyen, D. T.; Case, D. A. *J. Comput. Chem.* **1986**, *7*, 230.
 (33) McDonald, D. Q.; Still, W. C. *Tetrahedron Lett.* **1993**, *33*, 7743.
 (34) Still, W. C.; Tempezyk, A.; Hawley, R. C.; Hendrickson, T. *J. Am. Chem. Soc.* **1990**, *112*, 6127.
 (35) Qiu, D.; Shenkin, P. S.; Hollinger, F. P.; Still, W. C. *J. Phys. Chem. A* **1997**, *101*, 3005.
 (36) Tarkoy, M.; Phipps, A. K.; Schultze, P.; Feigon, J. *Biochemistry* **1998**, *37*, 5810–5819.
 (37) Shields, G. C.; Laughton, C. A.; Orozco, M. *J. Am. Chem. Soc.* **1997**, *119*, 7463–7469.
 (38) Chang, G.; Guida, W. C.; Still, W. C. *J. Am. Chem. Soc.* **1989**, *111*, 4379.
 (39) Kolossvary, I.; Guida, W. C. *J. Comput. Chem.* **1993**, *14*.

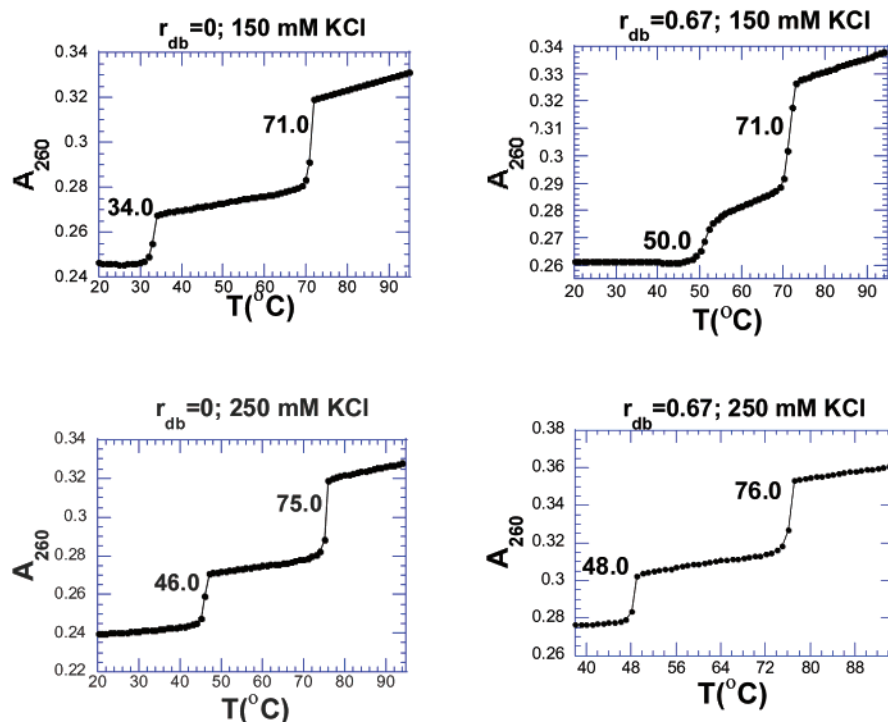


Figure 2. UV melting profiles of PolydA·2PolydT at the indicated r_{db} (ratio of neomycin/base triplet) and KCl concentrations. [DNA] = 15 μ M/base triplet. Buffer conditions: 10 mM sodium cacodylate buffer, 0.5 mM EDTA, pH 7.2.

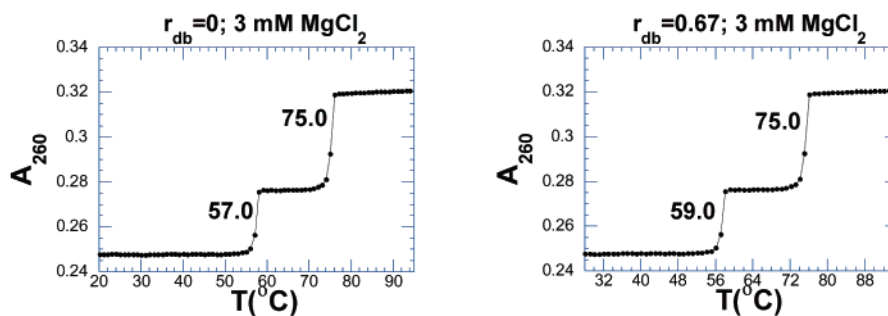


Figure 3. UV melting profiles of PolydA·2PolydT at the indicated r_{db} (ratio of neomycin/base triplet) and $MgCl_2$ concentration in the presence of 150 mM KCl. [DNA] = 15 μ M/base triplet. Buffer conditions: 10 mM sodium cacodylate buffer, 0.5 mM EDTA, pH 7.2.

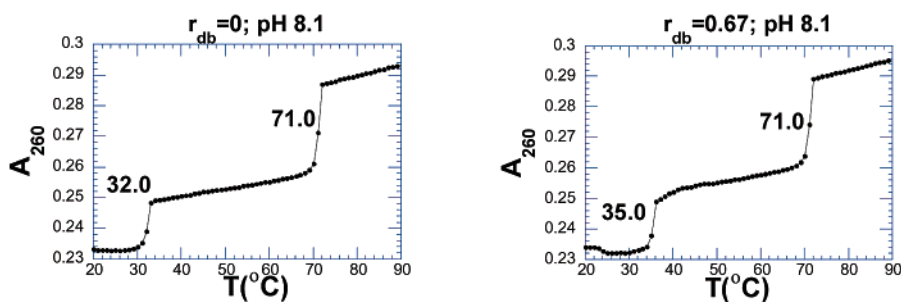


Figure 4. UV melting profiles of PolydA·2PolydT at the indicated r_{db} (ratio of neomycin/base triplet) and pH in the presence of 150 mM KCl. [DNA] = 15 μ M/base triplet. Solution conditions: 10 mM sodium cacodylate buffer, 0.5 mM EDTA, pH 7.2.

pH decreases the stabilization induced by neomycin. For the polynucleotide triplex, there is a decrease in $\Delta T_{m3\rightarrow 2}$ from 16 $^{\circ}C$ (pH 7.2) to 3 $^{\circ}C$ (pH = 8.1), suggesting a complete loss of neomycin's effectiveness in stabilizing the triplex, as the pH of the solution approaches above the pK_a values of neomycin amines.

D. Viscosity Changes as a Measure of Mode of Drug Binding. The viscosity of the polydA·2polydT triplex with increasing concentrations of neomycin was investigated to

understand the mode of drug interaction. More widely reported drug binding using viscosity techniques has involved the use of intercalating drugs.^{40–44} A relative increase in nucleic acid

- (40) Lee, J. S.; Waring, M. J. *Biochem. J.* **1978**, *173*, 115–128.
- (41) Fox, K. R.; Gauvreau, D.; Goodwin, D. C.; Waring, M. J. *Biochem. J.* **1980**, *191*, 729–742.
- (42) Satyanarayana, S.; Dabrowiak, J.; Chaires, J. *Biochemistry* **1993**, *32*, 2573–2584.
- (43) Luck, G.; Reinert, K. E.; Baguley, B.; Zimmer, C. J. *Biomol. Struct. Dyn.* **1987**, *4*, 1079–1094.

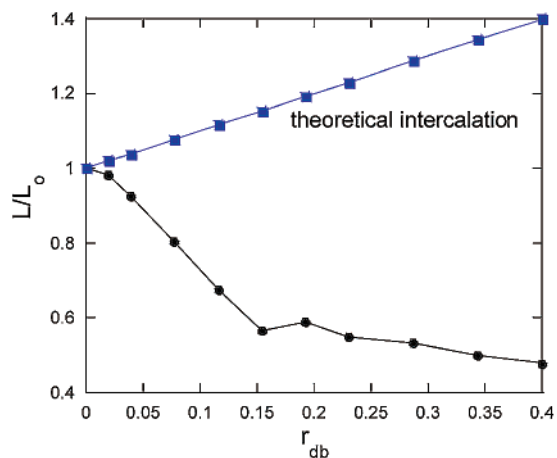


Figure 5. Change in PolydA·2PolydT DNA triplex solution viscosity upon increasing neomycin concentration. [DNA] = 100 μ M/base triplet. Buffer conditions: 10 mM sodium cacodylate, 0.5 mM EDTA, 150 mM KCl, 2.5 mM MgCl₂, pH 7.2. All solutions (buffer, nucleic acid, drug) contained identical buffer/salt concentrations to avoid any artificial differences in viscosity. r_{db} = ratio of the drug/base triplet.

solution viscosity is observed as a result of the intercalating event: an increased length in the nucleic acid from the classical intercalation mode of binding, which results in an overall increase in the solution viscosity.⁴⁵ While intercalating compounds have displayed this phenomenon, groove binding drugs such as berenil/tobramycin have been shown to induce a decrease in DNA/RNA solution viscosity.^{46,47} Such an event can be described by a bend or loop within the DNA helix, shortening the overall helical length.⁴⁵ A similar decrease in viscosity was observed in neomycin's interaction with the polydA·2polydT triplex. However, to avoid precipitation of the complex, the viscosity measurements had to be carried out with reduced DNA triplet concentration (100 μ M/base triplet, which is lower than normally used in these assays),^{46,47} as well as an increased MgCl₂ concentration (Figure 5). Upon increasing neomycin concentration, we observed a marked decrease in solution viscosity. As previously suggested, a bending within the triple helix (from groove binding) can lead to the resulting "rodlike" shortening of the DNA, in turn decreasing the DNA solution viscosity. This result suggests strong groove binding between neomycin and the polydA·2polydT triplex with negligible duplex interaction (otherwise typical of intercalation or less specific groove binding drugs), which has received considerable attention by other biophysical methods such as UV thermal denaturation and isothermal kinetic analysis.

3. Neomycin Binding to a Smaller dA₁₆·2dT₁₆ Triplex.

While neomycin can effectively stabilize a polynucleotide triplex, it was of interest to investigate its effects on shorter sequences. We carried out thermal denaturation studies of a dA₁₆·2dT₁₆ triplex. In the absence of drug, a transition for this triplex is not observed (150 mM KCl, pH = 6.8, 10 mM sodium cacodylate, 0.5 mM of EDTA, UV or CD melts), even when the dT₁₆ and dA₁₆ strands are mixed in a 2:1 ratio. Upon addition

of small amounts of neomycin, a clear T_{m3-2} transition becomes visible at 31 °C, while the duplex transition is not affected (Figure 6a). The presence of a triplex under these conditions was further verified by a Job plot in the presence of the drug. A clear minimum is seen at 66% of dT₁₆ suggesting the formation of triplex (Figure 6b). No other aminoglycoside was able to induce triplex formation under such small drug concentrations (r_{db} = 0.67, Figure 6c).

Salt and pH dependent studies were then carried out for the dA₁₆·2dT₁₆ triplex, and an effect similar to that with polynucleotide triplex was observed (drug competition with increasing pH and KCl and MgCl₂ concentrations). At a fixed drug concentration (r_{db} = 0.67), the following effects are observed: (i) When the pH is raised from 7.2 to 8.2, T_{m3-2} decreases from 31 °C to 11 °C, whereas T_{m2-1} is unaffected. Figure 7 shows this effect of neomycin on triplex and duplex T_m in greater detail as the pH is raised from 5.9 to 8.2. Below pH 6.5, there is some nondiscriminate binding of the drug to the duplex as well as triplex, but, above pH 6.5, triplex T_{m3-2} is the only transition that is influenced by a change in pH. (ii) There is a decrease in T_{m3-2} from 31 °C (150 mM KCl) to 2 °C (250 mM KCl). (iii) There is a decrease in T_{m3-2} from 31 °C (no MgCl₂) to 29 °C (3 mM MgCl₂).

There is an induction of triplex at 3 mM MgCl₂, with a T_{m3-2} of 6 °C (Supporting Information). This allows us to look at ΔT_{m3-2} in the absence and presence of drug. As opposed to the polynucleotide triplex, where ΔT_{m3-2} is reduced to 2 °C (0–3 mM MgCl₂), neomycin can still stabilize the triplex considerably (ΔT_{m3-2} = 23 °C). This difference may reflect the potential/shape difference in pockets of negative charge that exist in the polynucleotide versus the 16mer triplex. MgCl₂ can displace neomycin from the polynucleotide triplex much more effectively than it can from the smaller oligomer.

4. CD Spectroscopy. Number of Base Triplets/Drug.

Binding induced changes in a nucleic acid's CD spectrum can be exploited to determine binding stoichiometry between ligand and its host nucleic acid.^{46–49} Recently, Pilch has shown that CD-detected binding of tobramycin to RNA can be used for determining the binding site size of bound tobramycin and that this apparent binding site size can be used in further calculations for profiling the thermodynamics of tobramycin–RNA recognition.⁴⁷ Our initial efforts were to study the effect of neomycin upon the CD spectrum of the polynucleotide TAT triplex. However, there was found to be very little change in CD signal of the nucleic acids upon increasing concentration of the drug. The change in CD signal is dependent upon the pH as well as salt concentrations (lower pH and salt concentrations showing the maximum effect). Additionally, we have used an intramolecular triplex 5'-dA₁₂-x-dT₁₂-x-dT₁₂-3' to calculate the binding site size. The CD titration and plot of this triplex with increasing neomycin concentration is shown in Figure 8a. The binding site size is ~6 base triplets/drug. At higher drug concentrations, CD changes reflect an additional binding site at 2 base triplets/drug. With the mixed base 22mer triplex previously studied by us,¹² a larger change in CD signal is observed (Supporting Information). A plot of normalized molar ellipticity versus $1/r_{db}$ is shown in Figure 8b, suggesting a binding site size of ~7 base triplets/drug.

(44) Fox, K. R.; Olsen, R. K.; Waring, M. J. *Br. J. Pharmacol.* **1980**, *70*, 25–40.

(45) Suh, D.; Chaires, J. B. *Bioorg. Med. Chem.* **1995**, *3*, 723–728.

(46) Pilch, D. S.; Kirolos, M. A.; Liu, X.; Plum, G. E.; Breslauer, K. J. *Biochemistry* **1995**, *34*, 9962–9976.

(47) Jin, E.; Katritch, V.; Olson, W. K.; Kharatisvili, M.; Abagyan, R.; Pilch, D. S. *J. Mol. Biol.* **2000**, *298*, 95–110.

(48) Pilch, D. S.; Kirolos, M. A.; Breslauer, K. J. *Biochemistry* **1995**, *34*, 16107–16124.

(49) Rentzeperis, D.; Marky, L. A. *J. Am. Chem. Soc.* **1995**, *117*, 5423–5424.

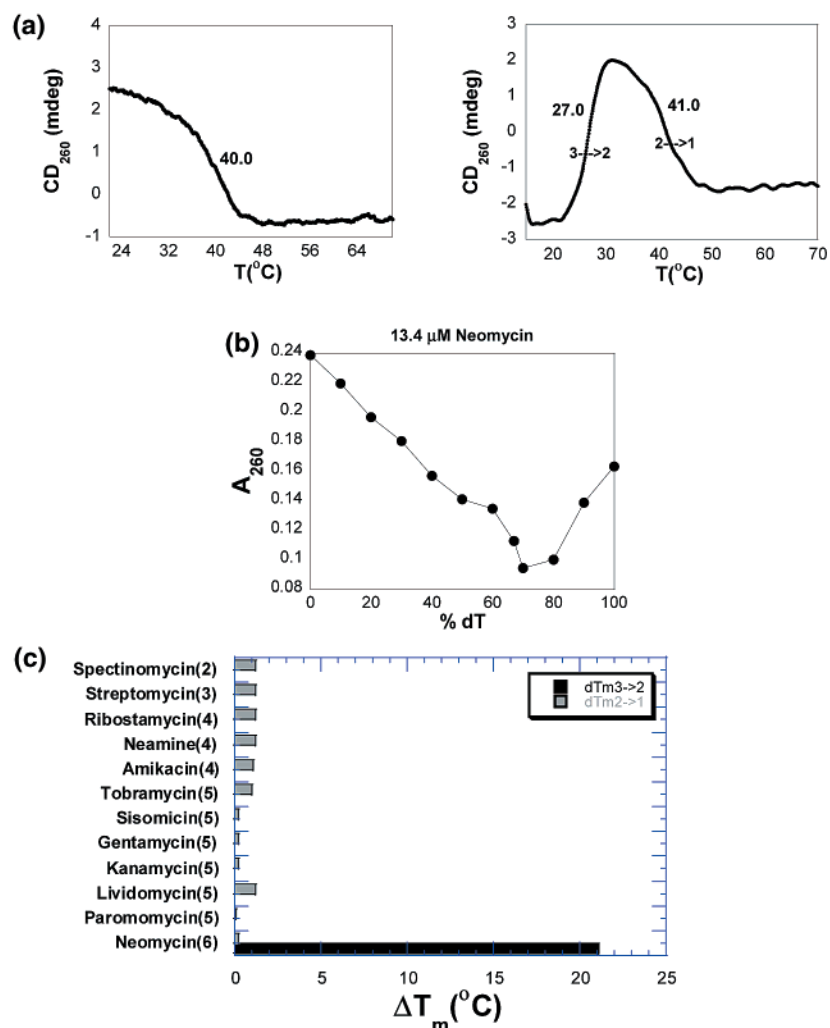


Figure 6. (a) CD melting profiles of dA₁₆·2dT₁₆ in the absence (left) and presence (right) of neomycin. [DNA] = 1.25 μM/strand (20 μM/base triplet). Solution conditions: 150 mM KCl, 10 mM sodium cacodylate buffer, 0.5 mM EDTA, pH 7.2. The sample was heated to 95 °C for 5 min, cooled to ambient temperature, and incubated at 4 °C for 16 h. (b) Job plot of dA₁₆ (1.25 μM/strand) and dT₁₆ (1.25 μM/strand) with neomycin at 10 °C showing a minimum at ~66% of dT₁₆. Solution conditions: 150 mM KCl, 10 mM sodium cacodylate buffer, 0.5 mM EDTA, pH 7.2. (c) Effect of added aminoglycoside ($r_{db} = 0.67$) on inducing the 16mer triplex dA₁₆·2dT₁₆ formation. Number of amines in each aminoglycoside is shown in parentheses. ΔT_{m3-2} is calculated by assuming a T_{m3-2} of 10 °C in the absence of neomycin (no transition seen).

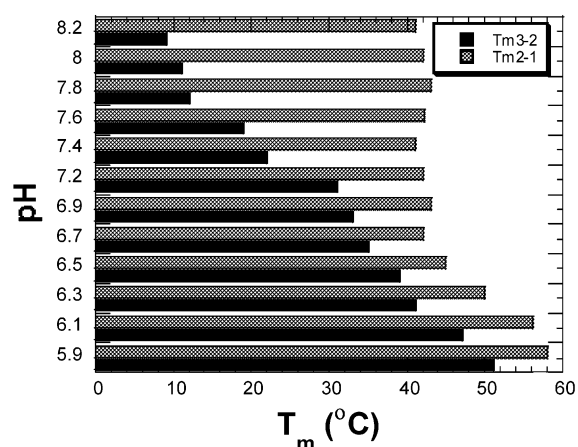


Figure 7. Variation in triplex (T_{m3-2}) and duplex (T_{m2-1}) melting points of dA₁₆·2dT₁₆ at the indicated pH in the presence of 150 mM KCl. [DNA] = 20 μM/base triplet; [Neomycin] = 13.4 μM. Buffer conditions: 10 mM sodium cacodylate buffer, 0.5 mM EDTA.

As mentioned previously, ligand induced changes in the CD spectrum of host DNA can assist in determining apparent

binding site sizes. It is important to mention that, in cases where more than one inflection point is observed (in single wavelength plots, normalized molar ellipticity versus $1/r_{db}$), it is not possible to differentiate whether the observed change is a result of multiple, separate binding motifs or of conformational changes induced by the ligand upon saturating a single binding motif.⁴⁸ However, viscosity experiments with polymeric DNA, as mentioned earlier, suggest a nonintercalative mode of binding, which prompts us to believe that lower binding site sizes, such as that observed with the intramolecular triplex (Figure 8a), can be a result of cooperative binding or drug stacking at the exterior of the helix.⁴⁸ Our ITC experiment also suggests the presence of a six base triplet/drug binding site as the key high affinity site (shown later).

5. Specificity in Drug Binding to a DNA Triplex (Effect of Increasing C Content). Thermal denaturation studies of polydG·2polydC with neomycin were carried out for comparison of triplex stabilization versus polydA·2polydT. We have found that neomycin stabilizes polydG·2polydC ($\Delta T_m = 11$ °C) at $r_{db} = 1.67$, but the degree of stabilization is limited when compared to polydA·2polydT ($\Delta T_m = 24.7$ °C).

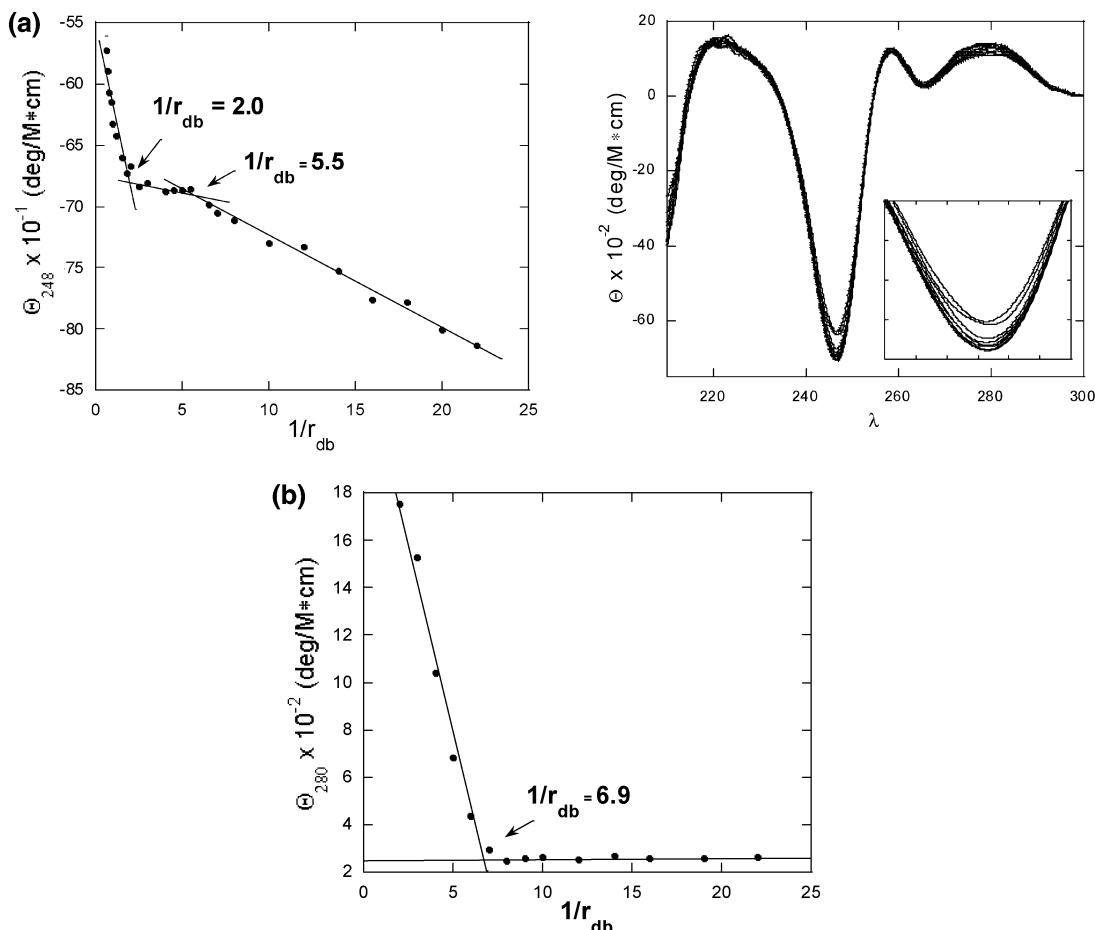


Figure 8. (a) A plot of normalized molar ellipticity vs $1/r_{db}$ (left) for CD titration of 5'-dA₁₂-x-dT₁₂-x-dT₁₂-3' triplex with neomycin. CD titration curve (right) of neomycin and 5'-dA₁₂-x-dT₁₂-x-dT₁₂-3' triplex. The insert in the right plot is an expanded spectrum from 240 to 255 nm. For clarity, not all the CD spectra are shown. The continuous lines in the left plot reflect the linear least-squares fits of each apparent linear domain of the experimental data (●) before and after the apparent inflection point. Molar ellipticity is per molar base triplet, and r_{db} = ratio of the drug/base triplet. Buffer conditions: 10 mM sodium cacodylate, 0.5 mM EDTA, 150 mM KCl, pH 6.8. (b) A plot of normalized molar ellipticity vs $1/r_{db}$ for CD titration of the dY₂₂dR₂₂dT₂₂ triplex with neomycin. The continuous lines in the left plot reflect the linear least-squares fits of each apparent linear domain of the experimental data (●) before and after the apparent inflection point. Molar ellipticity is per molar base triplet, and r_{db} = ratio of the drug/base triplet. Buffer: 10 mM sodium cacodylate, 0.1 mM EDTA, pH 6.80; [KCl] = 150 mM.

It is noteworthy to mention that both triplex (polydG·2polydC and polydA·2polydT) melting temperatures are nearly identical in the presence of a high concentration of neomycin ($r_{db} = 1.67$). This suggests that, under the conditions studied, neomycin concentrations are necessarily high such that DNA melting occurs at a consistent temperature independent of sequence. Binding of neomycin thus occurs at sites containing CGC⁺ triplets as well as TAT triplets.

Two intramolecular triplexes (5'-dA₁₂-x-dT₁₂-x-dT₁₂-3' and 5'-AAAGAAAAGAAA-x-TTTCTTTTCTTT-x-TTTCTTTTCTTT-3') were also used to study the effect on neomycin's effectiveness of adding CGC⁺ triplets. In the absence of neomycin, melting temperatures of these intramolecular triplexes are 30 °C and 46 °C at 100 mM KCl, respectively. Insertion of CGC⁺ triplets into AT tract sequences increases the native melting temperature by 16 °C which is consistent with the results previously reported.⁵⁰ In the presence of neomycin at 100 mM KCl, the stability of both intramolecular triplexes has been observed. As shown in Figure 9c, the degree of stabilization on 5'-dA₁₂-x-dT₁₂-x-dT₁₂-3' is 15 °C higher than that on 5'-

AAAGAAAAGAAA-x-TTTCTTTTCTTT-x-TTTCTTTTCTTT-3' at $r_{db} \approx 0.6$. This observation clearly suggests that neomycin stabilizes both TAT and CGC⁺ rich sequences but favors TAT triplets. A smaller but similar trend is seen at higher salt concentration (150 mM KCl, Figure 9c). In the presence of neomycin, duplex melting temperatures are unperturbed, suggesting no effect of neomycin on the intramolecular duplex under the condition studied (see Supporting Information).

We then synthesized six additional DNA sequences (22mers) with varying C content. The 22-base sequences, shown in Scheme 2, were chosen as they are able to exhibit triplex melting in the absence of drug. (An exception is the dT₂₂ containing sequence, of which no triplex melting was detected in the absence of drug.) This change in $T_{m3 \rightarrow 2}$ is plotted as a function of cytosine percentage in Figure 9d. These comparisons could only be made at high drug concentrations, as biphasic transitions are observed with these mixed base sequences at lower neomycin concentration. All triplexes showed a ΔT_m between ~45 and 50 °C. As shown in Figure 9d, the triplex T_m for all 22mer sequences in the presence of neomycin remains fairly consistent, with the native triplex displaying variations in T_m dependent on C content and adjacent CGC⁺ triplets. This

(50) Sandstrom, K.; Warmlander, S.; Graslund, A.; Leijon, M. *J. Mol. Biol.* **2002**, *315*, 737–748.

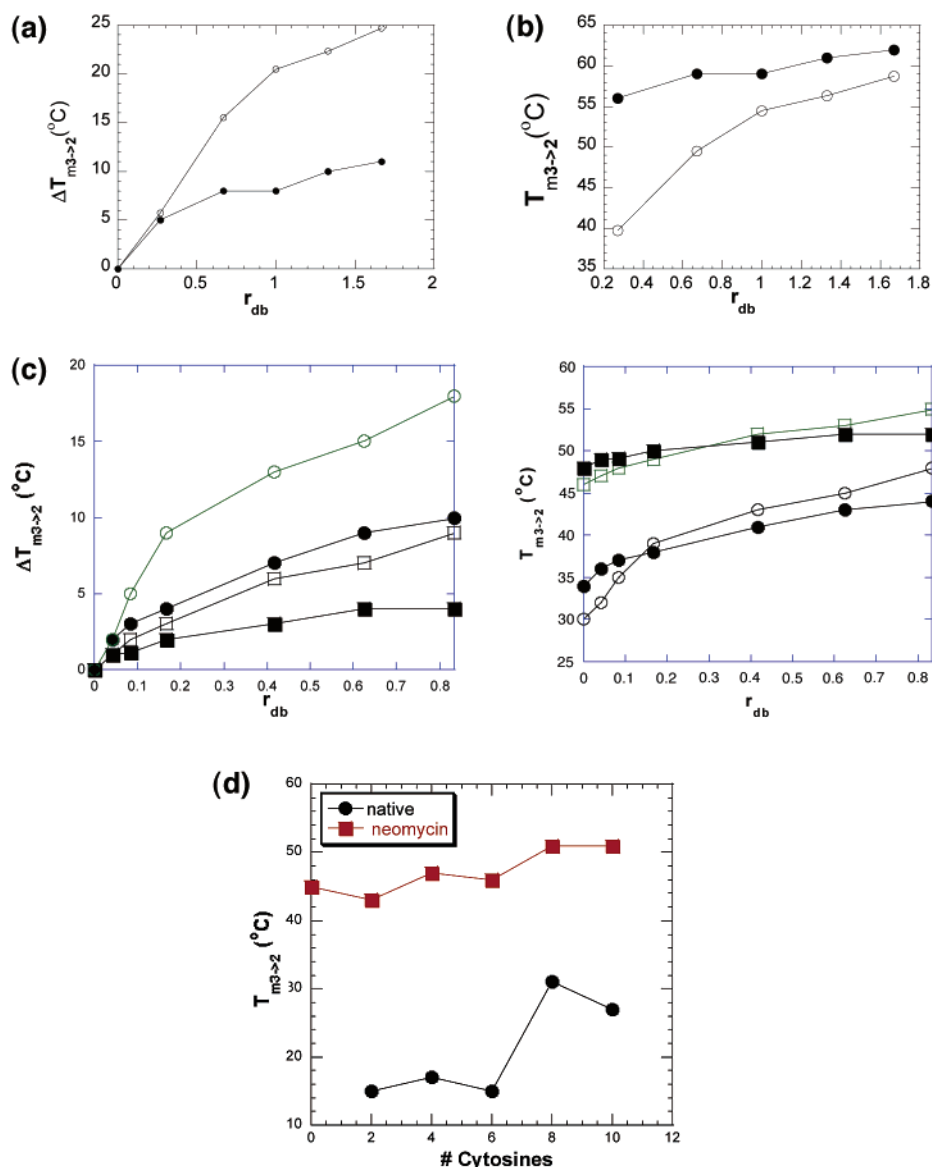


Figure 9. A plot of variation of $\Delta T_{m3 \rightarrow 2}$ (a) and $T_{m3 \rightarrow 2}$ (b) of polydG·2polydC (●) and polydA·2polydT (○) as a function of increasing neomycin concentration in the presence of 150 mM KCl. [DNA] = 15 μ M/base triplet, pH = 6.8 (for the triplex polydG·2polydC) and 7.2 (for the triplex polydA·2polydT), 10 mM sodium cacodylate buffer, 0.5 mM EDTA. r_{db} = ratio of drug/base triplet. (c) Plots of $\Delta T_{m3 \rightarrow 2}$ (left) and $T_{m3 \rightarrow 2}$ (right) of 5'-dA₁₂-x-dT₁₂-x-dT₁₂-3' {in the presence of 100 mM KCl (○) and 150 mM KCl (●)} and 5'-AAAGAAAAGAAA-x-TTCTTTTCTTT-x-TTCTTTTCTTT-3' {in the presence of 100 mM KCl (□) and 150 mM KCl (■)} as a function of increasing neomycin concentration [r_{db} = drug(neomycin)/base triplet ratio]. [DNA] = 2 μ M/strand, pH = 6.8, 10 mM sodium cacodylate buffer, 0.5 mM EDTA. (d) Variation in the triplex ($T_{m3 \rightarrow 2}$) melting point of various 22mer DNA triplexes (with varying C content) at the indicated drug r_{db} = 0.67, in the presence of 150 mM KCl. [DNA] = 15 μ M base triplet, pH = 6.8, 10 mM sodium cacodylate buffer, 0.5 mM EDTA. UV melt not observed with the dT₂₂ triplex (Scheme 2, triplex 1) in the absence of neomycin.

Scheme 2. Base Sequences of Triplex Forming Oligonucleotide (TFO) Third Strands Used in the Study^a

1. TTTTTTTTTTTTTTTTTTTTTTTT
2. TTCTTTTTTTTTTTTTTTTCTT
3. TTCCTTTTTTTTTTTTTTCCCTT
4. TTCCCTTTTTTTTTTTCCCTT
5. TTCCCTTTCTTTTCTTTCCCTT
6. TTCCCTTTCTTTCTTTCCCTT

^a The corresponding purine·pyrimidine duplexes are not shown for brevity.

observation remains consistent with results obtained for polymeric CGC⁺ triplex, that regardless of base makeup the triplex

under the influence of high neomycin concentration results in a similar T_m .

6. Thermodynamics of Neomycin Binding to the PolydA·2PolydT Triplex, as Determined using Isothermal Titration Calorimetry. We used isothermal titration calorimetry (ITC)^{51–55} to characterize the binding of neomycin to intramolecular triplex (5'-dA₁₂-x-dT₁₂-x-dT₁₂-3') in cacodylate buffer at a constant K⁺ concentration of 150 mM. Figure 10a shows the representative ITC profile resulting from the injection of neomycin into a

- (51) Haq, I.; Chowdhry, B. Z.; Jenkins, T. C. *Methods Enzymol.* **2001**, *340*, 109–149.
- (52) Haq, I.; Ladbury, J. E.; Chowdhry, B. Z.; Jenkins, T. C. *J. Am. Chem. Soc.* **1996**, *118*, 10693–10701.
- (53) Haq, I.; Ladbury, J. *J. Mol. Recognit.* **2000**, *13*, 188–197.
- (54) Haq, I.; Jenkins, T. C.; Chowdhry, B. Z.; Ren, J.; Chaires, J. B. *Methods Enzymol.* **2000**, *323*, 373–405.
- (55) Doyle, M. L.; Hensley, P. *Methods Enzymol.* **1998**, *295*, 88–364.

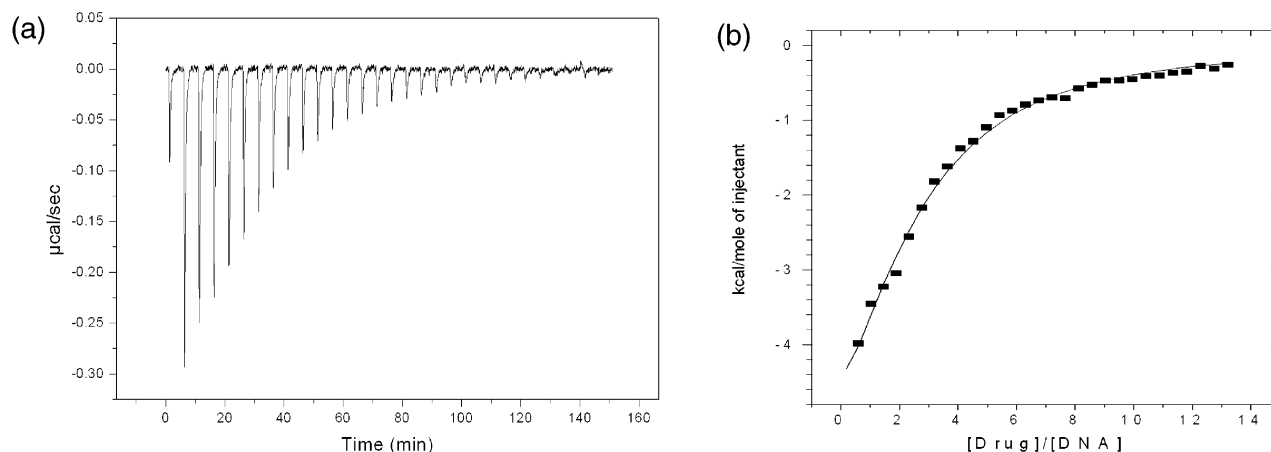


Figure 10. (a) ITC profile of 5'-dA₁₂-X-dT₁₂-X-dT₁₂-3' (4 μ M/strand) titrated with neomycin (500 μ M) in 10 mM sodium cacodylate, 0.5 mM EDTA, and 150 mM KCl, pH 6.8 at 20 °C. (b) Corrected injection heats plotted as a function of the [drug]/[DNA] ratio. The corrected injection heats were derived by integration of the ITC profiles shown in Figure 10a, followed by subtraction of the corresponding dilution heats derived from control titrations of drug into buffer alone. The data points reflect the experimental injection heats, while the solid line reflects calculated fit of the data.

Table 1. ITC Derived Thermodynamic Profiles for the Binding of Neomycin to the 5'-dA₁₂-X-dT₁₂-X-dT₁₂-3' Triple Helix in 10 mM Sodium Cacodylate, 0.5 mM EDTA, and 150 mM KCl, pH 6.8 at 20 °C

<i>T</i> (K)	<i>K</i> ($\times 10^5$ M ⁻¹)	ΔH (kcal mol ⁻¹)	$T\Delta S$ (kcal mol ⁻¹)	ΔG (kcal mol ⁻¹)	<i>N</i> (drug/triplex)
293	1.96 \pm 0.13	-6.9 \pm 0.3	0.18	-7.1 \pm 0.04	2.17 \pm 0.09

solution of 5'-dA₁₂-X-dT₁₂-X-dT₁₂-3'. Each of the heat burst curves in Figure 10a corresponds to a single drug injection. The areas under these heat burst curves were determined by integration to yield the associated injection heats.

These injection heats were corrected by subtraction of the corresponding dilution heats derived from the injection of identical amounts of drug into buffer alone. Figure 10b shows the resulting corrected injection heats plotted as a function of the [drug]/[DNA] ratio. In this figure, the data points reflect the experimental injection heats, while the solid line reflects the calculated fit of the data. The injection heat data corresponding to the titration of the triplex DNA with neomycin were fit with a model for a single binding site. With the resulting values of *K*_a, we calculated the corresponding binding free energy. The binding free energy, coupled with the binding enthalpy derived from the fitted ITC data, allowed us to calculate the corresponding entropic contributions to binding ($T\Delta S$; where ΔS is the binding entropy). These analyses allowed us to derive the thermodynamic binding profile summarized in Table 1.

The best fit of the data was to a single binding site, yielding an association constant of $\sim 2 \times 10^5$ M⁻¹. The reaction which is exothermic, as also visible from the ITC profile, proceeds by little change in entropy and yields a binding site of ~ 6.0 base triplets/drug, which is 2 drugs/strand (Table 1, *N* \approx 2). The smaller and perhaps weaker binding site of 2 base triplets is not observed even at higher drug concentrations in the ITC study. The high affinity of neomycin is primarily, if not entirely, enthalpic in origin. A much larger binding constant is observed with the polynucleotide triplex ($\sim 10^7$ M⁻¹), suggesting possible cooperativity in binding to the larger polydA \cdot 2polydT triplex (Supporting Information).

7. Modeling Studies/Discussion. The minor groove binders have little preference for the DNA triple helix (berenil,

distamycin, and Hoechst dyes).¹² Most groove binders stabilize the duplex much more effectively.^{56,57} A few even destabilize the triplex.^{9,12} Neomycin does not affect the DNA duplex even at concentrations higher than that shown in Figure 1. Molecular dynamics (MD) simulations have been effectively used by Orozco et al. to study the dynamical and time-averaged characteristics of the DNA triple helix dA₁₀ \cdot 2dT₁₀.³⁷ The minor groove (W–C groove) of the triplex is similar in width and depth to that of B-type duplex DNA and does not resemble at all the minor groove of an A-type or P-type triplex DNA.^{37,58} The shortest average distance between phosphates across this groove is around 11–12 Å which gives a groove width of 5.8 Å, matching typical values for B-type duplex DNA (5.9 Å). However, while the B-form duplex minor groove has a U-shaped cross section, the triplex minor groove has a V-shaped cross section. Thus, while some established duplex minor-groove binding ligands such as netropsin and distamycin can bind to triple helices, they destabilize them as they bind more strongly to the duplex generated on loss of the triplex-forming strand.⁹ The major groove is quite different from that in standard B-type DNA, since the presence of the third strand widens the major groove and divides it into two asymmetric parts: the minor part of the major groove (Crick–Hoogsteen (C–H) groove) and the major part of the major groove (Watson–Hoogsteen (W–H) groove). Inspection of the W–H groove shows the existence of three possible H-bond donors and acceptors in the bottom of the groove: N6(A), O4(T–WC), and O4(T–Hoogsteen). However, all three are buried behind the two methyl groups of thymine at C5, which may impede (but does not preclude) their accessibility to interacting molecules. The W–H groove is wide enough to interact with such molecules as neomycin and has very different requirements for sequence-specific recognition than the major groove of duplex B-DNA.

As observed previously,^{36,37,58} both the W–C and the C–H grooves are quite rigid due to the existence of highly structured water molecules in both grooves. In contrast to the smaller grooves, the W–H groove is quite flexible, making possible

(56) Sarma, M. H.; Umemoto, K.; Gupta, G.; Luo, J.; Sarma, R. H. *J. Biomol. Struct. Dyn.* **1990**, *8*, 461–482.

(57) Durand, M.; Thuong, N. T.; Maurizot, J. C. *J. Biomol. Struct. Dyn.* **1994**, *11*, 1191–1202.

(58) Radhakrishnan, I.; Patel, D. J. *Structure* **1994**, *2*, 17–32.

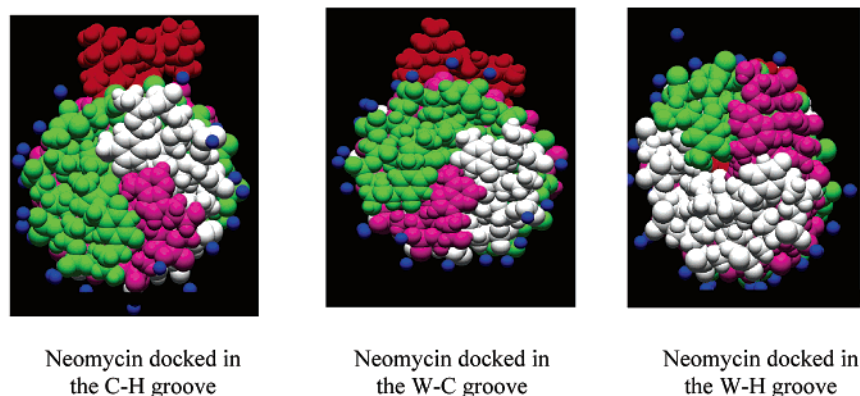


Figure 11. Computer generated model showing aerial view of neomycin (red) bound to three different grooves of the TAT DNA triplex. Neomycin is almost invisible when docked into the Watson–Hoogsteen groove.

expansions and contractions of the groove greater than 2 Å from the average values. This large flexibility could be used by the DNA triplex to adapt its shape to a conformationally restrained molecule like neomycin. Inspection of other helical parameters has previously shown that these groove movements are not clearly connected to any change in particular helical parameters, which implies that W–H groove flexibility does not lead to major alterations in the general shape of the triplex.^{36,37}

It has already been shown that Dst2, a distamycin analogue, binds specifically to the minor groove (Watson–Crick groove) of the $dA_6 \cdot 2dT_6$ triplex.^{56,59} This is not surprising because distamycin prefers the DNA duplex and destabilizes the DNA triplex.^{12,60,61} The wider size of the Watson–Hoogsteen groove remains as the most likely binding site for a triplex groove selective agent (neomycin). Our experimental evidence conclusively shows that neomycin (and even some of its conjugates) stabilizes the triplex but not the duplex.^{12,62} Ligands that stabilize the duplex better than triplex (like distamycin) can be expected to bind in the Watson–Crick groove rather than the Watson–Hoogsteen groove (as reported).⁵⁹ For selective triplex stabilization, however, the Watson–Hoogsteen groove must be targeted.⁴⁹

The neomycin molecule, in water, was highly flexible, especially in ring III and IV regions. Sixteen conformations were found within a 12 kJ/mol range above the global minimum, and 42, within a 20 kJ/mol range above the global minimum. A few of these structures are shown in the Supporting Information. The neomycin molecule, in five of its conformations, was then manually docked to the DNA triplex grooves (Watson–Hoogsteen, Watson–Crick, and Crick–Hoogsteen; Figure 11). The structure–activity relationship available from natural product binding (Figure 1, also supporting info) was used to specify ring I and ring IV amines as the key components in binding. Our hypothesis that neomycin binds in the Watson–Hoogsteen groove is substantiated by looking at the aerial view of the triplex with neomycin docked into the 3 grooves (Figure 11). As clearly seen, neomycin becomes almost invisible when docked into the Watson–Hoogsteen groove, whereas one or two neomycin rings are always seen lying outside the other two

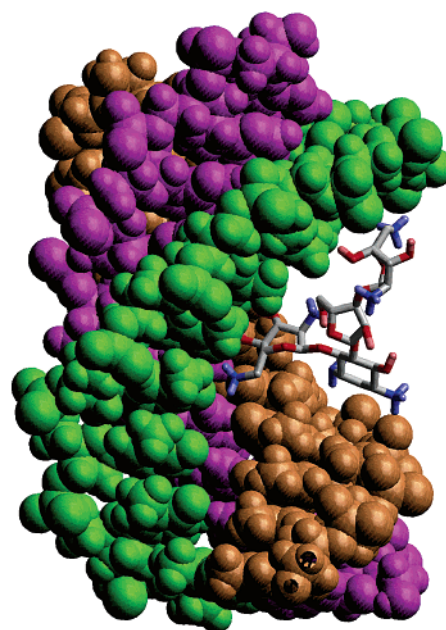


Figure 12. Computer generated model of neomycin bound to a W–H groove of a DNA triplex. Neomycin ring I sits in the center of the groove, while the amines on rings II and IV help bridge the two pyrimidine strands together.

triplex grooves (Crick–Hoogsteen; Watson–Crick). In Figure 12, a side view of neomycin bound to the W–H groove is shown. Six new H-bonds are formed when neomycin binds the Watson–Hoogsteen groove of the DNA triplex (among neomycin amines, hydroxyl and thymidine O3, and phosphate oxygen, respectively). Four H-bonds are formed when neomycin binds in the Crick–Hoogsteen groove, and three, in the Watson–Crick groove. This remarkable recognition is similar, in principle, to aminoglycoside recognition of RNA aptamers, where specificity is achieved by the encapsulation of up to 75% of the drug surface in the accessible target cavity.⁶³

Electrostatic potential maps show a large concentration of negative potential along sterically permitted regions within the three grooves. All three grooves can be targets for interactions with positively charged groups, and at first glance, the minor grooves appear to be better targets than the W–H groove (more concentrated negative charge; see Figure 13).³⁷ The shape/charge

(59) Umemoto, K.; Sarma, M. H.; Gupta, G.; Luo, J.; Sarma, R. H. *J. Am. Chem. Soc.* **1990**, *112*, 4539–4545.

(60) Durand, M.; Maurizot, J. C. *Biochemistry* **1996**, *35*, 9133–9139.

(61) Durand, M.; Thuong, N. T.; Maurizot, J. C. *J. Biol. Chem.* **1992**, *267*, 24394–24399.

(62) Xue, L.; Charles, I.; Arya, D. P. *J. Chem. Soc., Chem. Commun.* **2002**, 70–71.

(63) Jiang, L.; Majumdar, A.; Hu, W.; Jaishree, T. J.; Xu, W.; Patel, D. J. *Structure* **1999**, *7*, 817–827.

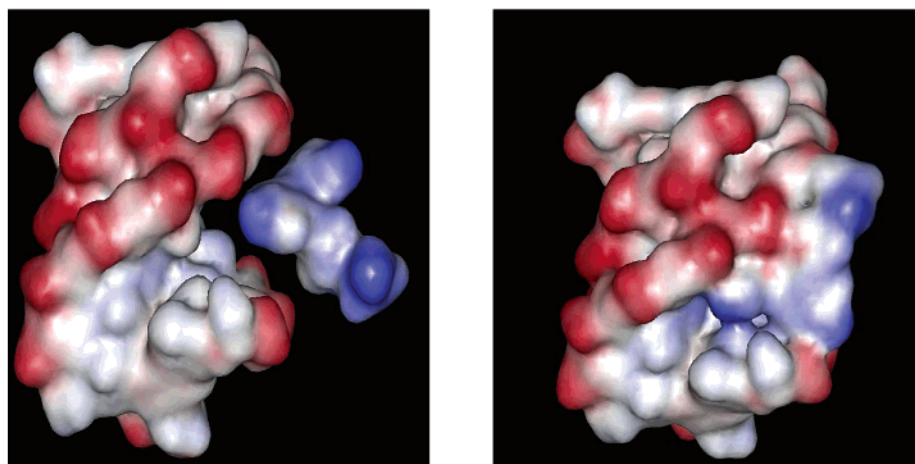


Figure 13. Charge/Shape complementarity of neomycin to the triplex W–H groove: electrostatic surface potential maps (left) of neomycin approaching the W–H groove of the triplex and (right) neomycin buried in the triplex groove.

complementarity of neomycin to the W–H groove, however, is largely responsible for its selectivity in triplex recognition (Figures 11 and 13). The selective binding of neomycin to the triplex is achieved in the presence of physiological salt (100–150 mM KCl). In the absence of salt, one observes indiscriminate binding to duplex/triplex backbones,¹² suggesting the importance of shape complementarity (Figure 11, 13) of neomycin to the W–H groove as a key factor in recognition (in the presence of KCl).

DNA based minor groove binders were the first to be examined for triplex DNA groove recognition, leading to limited successes, due in large part to the different structures of W–C grooves of the two molecules.⁹ Regular undistorted B-form helices of double stranded DNA do not mimic the structural recognition features present in triplex DNA.^{6,37} Among the various forces involved in such recognition processes, electrostatic interactions between the negatively charged triplex backbone and cationic groups are key in enhancing the binding affinity with drug complexes. However, a lack of spatial directionality leads to electrostatic forces that show nonspecific binding. Interaction of conformationally restrained antibiotics, with a combination of surface electrostatics and desired shape (such as aminoglycosides), can provide specific recognition to triplex DNA. Neomycin is shown here to be the first example that exhibits a spatial complementarity to triplex nucleic acid structures, similar to what has previously only been observed in RNA recognition by these antibiotics. Further studies (NMR and affinity cleavage) can now be used to probe the molecular contacts of this unique recognition.

The formation of a nucleic acid triplex into a scaffold of spatially oriented anionic groups creates pockets of focused negative charge. Such a distribution of charged pockets can provide a 3-D pattern that can be specifically targeted by compounds exhibiting structural electrostatic complementarity. Aminoglycosides are shown here to provide such scaffolds, where the positively charged ammonium groups displace several Mg²⁺ and K⁺ ions from their triplex binding sites. Such electrostatic complementarity has been successfully used to explain the structural basis of aminoglycoside inhibition of self-splicing group I introns.⁶⁴ The goal of achieving sequence

specific RNA recognition has similarly been shown to have more similarities to protein targets rather than a DNA duplex.²³ The 3-D structures of RNA aptamer complexes are able to encapsulate their substrate within a tightly fitting cavity. In a tobramycin–RNA aptamer complex, 75% of the accessible surface is buried inside the RNA fold.^{23,63} In complexes of aminoglycosides bound to natural targets, considerably less accessible surface of the drugs is buried relative to aptamers.²³ Perhaps the best complementarity for aminoglycosides with a natural target is observed with eubacterial ribosomal site A.²³ Our work (in concert with other reports) suggests that aminoglycoside binding may not be just RNA specific but specific for nucleic acids that can adopt the A-conformation (RNA duplex,^{11,12,24} A-form DNA duplex,²⁵ DNA–RNA hybrid duplex,¹¹ DNA triplex,¹² and RNA triplex¹²).

Pilch has recently calculated the ITC derived binding constant for aminoglycoside binding to a RNA duplex (10^6 – 10^7 M⁻¹)⁴⁷ and a higher binding constant (10^8 – 10^9 M⁻¹) for neomycin and aminoglycoside binding to RNA A-site.⁶⁵ These data were derived from a set of multiple binding sites at a salt concentration of 60 mM NaCl. Our work at 150 mM KCl yields an association constant of neomycin binding to a DNA triplex, which is an order of magnitude lower than that observed for neomycin binding to the RNA duplex. Since neomycin triplex association is favored by low salt, identical salt concentrations should give a higher K_a for neomycin–triplex.⁶⁶ Nevertheless, this high association of neomycin is unique for any triplex-specific groove binding agent observed to date. Even triplex-specific intercalators have been shown to have a binding constant similar to or lower than that of neomycin.⁵² With synthetic modifications, it should be possible to design ligands that can even compete with aminoglycoside binding to their natural targets—duplex RNA. A pyrene–neomycin conjugate has been previously shown by us to be much more effective than neomycin in stabilizing triplexes.⁶² A BQQ–neomycin conjugate binds nucleic acid triplexes with even higher affinity than the RNA A-site (unpublished results). Our work shows that neomycin's attraction for triplex grooves follows a recognition pattern similar to RNA/protein recognition and presents this

(65) Kaul, M.; Pilch, D. S. *Biochemistry* **2002**, *41*, 7695–7706.

(66) A complete pH and salt dependent thermodynamic (ITC/DSC) analysis of aminoglycoside interaction with the nucleic acid triplexes is currently under investigation and will be reported in due course.

(64) Hoch, I.; Berens, C.; Westhof, E.; Schroeder, R. *J. Mol. Biol.* **1998**, *282*, 557–569.

charge/shape complementarity of neomycin as a novel advance in the area of nucleic acid recognition. These interactions are triplex-specific (at physiological salt concentrations), leading to an overall stabilization of the triplex with respect to its “parent” duplex.

Summary

A large number of molecules have previously been studied for triplex recognition. The goal of triplex-selective groove recognition has so far remained elusive. Neomycin is shown to be the first molecule that can selectively stabilize DNA triplex structures (polynucleotides, small homopolymer, as well as mixed base triplexes). This stabilization is shown here to be based on neomycin’s ability to bind triplexes in the groove with high affinity (based on viscometric and ITC titrations). Modeling/physicochemical results suggest a further preference of

neomycin binding to the larger Watson–Hoogsteen groove. These findings will contribute to the development of a new series of triplex-specific (DNA/RNA and hybrid) ligands, which may contribute to either antisense or antigene therapies.

Acknowledgment. This study and the purchase of a VP-ITC was made possible by funds from NSF CAREER award to the PI:(CHE/MCB-0134932). We thank Prof. Jeff Petty (Furman University) for help with viscometric measurements.

Supporting Information Available: Structure/ pK_a ’s of aminoglycosides, thermal profiles, and conformations of neomycin. This material is available free of charge via the Internet at <http://pubs.acs.org>.

JA027765M